



Southern Hemisphere Sudden Stratospheric Warmings Continue to Be Relevant Under Global Warming

Sabine Bischof¹, Pia Undine Rethmeier^{1,2}, Wenjuan Huo¹, Sebastian Wahl¹, and Robin Pilch Kedzierski³

¹GEOMAR - Helmholtz Center for Ocean Research Kiel, Kiel, Germany

²Christian-Albrechts Universität Kiel, Kiel, Germany

³Department of Meteorology and Geophysics, Universität Wien, Vienna, Austria

Correspondence: Sabine Bischof (sbischof@geomar.de)

Abstract. In 2019, a stratospheric warming event strongly disrupted the stratospheric circulation in the Southern Hemisphere. This disruption led to negative anomalies in the Southern Annular Mode that propagated down to the troposphere and contributed to hotter and drier conditions in Australia, culminating in a devastating fire season. Although such events have been rare in the past, it remains unclear how climate change will affect their occurrence and surface impacts in the coming decades.

5 We conducted climate model time slice experiments to investigate how frequency and associated surface responses of Southern Hemispheric stratospheric warmings change under different global warming levels (present-day, 1.5 K, 2 K, 3 K, and 4 K). Additionally, we used an ensemble of historical experiments to confirm that our model simulations accurately capture the observed response to stratospheric warmings in the Southern Hemisphere. To investigate the change in stratosphere-troposphere coupling, we distinguish between downward- and non-propagating stratospheric events based on the Southern Annular Mode
10 response on different atmospheric levels. Our findings show that the frequency of major stratospheric warmings remains close to the historical frequency up to a warming of 2 K before decreasing more significantly. The coupling between the stratosphere and the troposphere shows a large decrease only at the 4 K warming level. Hence, as long as global warming levels remain at intermediate levels, the possibility of sudden stratospheric warmings contributing to extreme events continues to be relevant and would add to heat-related stress in Australia and Southern Africa, making adaptation to global warming more challenging.

15 1 Introduction

A sudden stratospheric warming (SSW), i.e. the breakdown of the prevailing stratospheric westerly circulation during winter and early spring, can have a significant impact on surface weather up to a few weeks after its onset in the stratosphere (Baldwin and Dunkerton, 2001). While SSWs occur almost every 1,5 years in the Northern Hemisphere (NH) they were very rare in the Southern Hemisphere (SH) with only two observed events, in 2002 and 2019 (Butler et al., 2017; Stolarski et al., 2005;
20 Safieddine et al., 2020). This difference between the hemispheres is due to differences in the mean states of the respective polar stratospheric vortices, mainly caused by a larger wave forcing on the NH (Shiotani and Hirota, 1985). To date, the 2002 event remains the only major SSW ever observed in the SH, i.e. the only one characterized by a reversal of the mean flow from westerly to easterly in the middle stratosphere at 10 hPa and 60° latitude, which is the most common criterion of a major SSW in the NH (Charlton and Polvani, 2007; Butler et al., 2015). Another strong disruption of the SH polar stratosphere,



25 characterized by an intense warming and deceleration of the westerly flow was observed in 2019 (Safieddine et al., 2020; Lim et al., 2021). Because the zonal mean zonal wind did not reverse to easterlies in this case, the event is referred to as a minor SSW. Nevertheless, this minor SSW had a large impact not only on stratospheric conditions but also on the surface, contributing to an extensive heat wave in Australia (Lim et al., 2021).

It was shown that the number of SH SSWs decreases significantly in a 4xCO₂ experiment compared to present-day conditions (Jucker et al., 2021). However, there has been no evaluation on the development of SSWs in the SH in the near future under more moderate warming conditions, nor has the increase in ozone been considered along with the changes in GHGs. This knowledge gap leads us to our first research question, which is to understand how SSW frequency will change under different global warming levels in the SH. Another open question we want to address in this publication is how the coupling characteristics and surface imprints of these events change under global warming.

35 To investigate the connection between the stratosphere and the troposphere, annular modes are often considered. These are the dominant modes of stratospheric as well as tropospheric variability in the high latitudes and nicely show the connection between the two atmospheric layers. On the SH, this variability pattern is called the Southern Annular Mode (SAM, Thompson and Wallace, 2000). Strong stratospheric vortex years are connected to a positive phase of the SAM, whereas weak stratospheric vortex years are connected to a negative phase of the SAM (Thompson et al., 2005; Dennison et al., 2015; Lim et al., 2018).
40 The coupling from the stratosphere to the troposphere is strongest in spring and summer and can lead to anomalies in the tropospheric SAM for up to 3 months after the onset of the stratospheric event (Thompson and Solomon, 2002; Thompson et al., 2005; Lim et al., 2018). The strong imprint of the stratospheric circulation anomalies in the tropospheric SAM implies that other climatic features sensitive to the tropospheric SAM also show a strong connection to these stratospheric anomalies. A negative tropospheric SAM, for example, is connected to an equatorward shift of the tropospheric jet, anomalous heat and a
45 lack of precipitation over Australia, anomalous cooling and enhanced precipitation over southern South America as well as to anomalous cooling over the eastern South African region (Lim et al., 2018, 2019). For positive SAM conditions, the opposite surface anomalies can be found.

In the last two decades of the 20th century, the stratospheric polar vortex was in a rather strong state caused by the depletion of stratospheric ozone due to anthropogenic emissions of chlorofluorocarbons and other halogen containing species on the one
50 hand and by the increase in anthropogenic greenhouse gases (GHGs) on the other hand (Thompson and Solomon, 2002). More precisely, ozone depletion led to decreased absorption of solar radiation in austral spring and rising GHG levels led to enhanced longwave cooling throughout the year for example by CO₂ (Rind et al., 1990; Randel and Wu, 1999). Both processes caused a cooling and an associated strengthening of the stratospheric polar vortex. The historical period of strong ozone depletion and GHG increase was therefore connected to a positive state of the SAM that even resulted in a poleward displacement of the
55 tropospheric jet (Thompson and Solomon, 2002; Gillett and Thompson, 2003). The tropospheric SAM trend, however, was only significant during late spring and summer, when the coupling between the stratosphere and the troposphere is the largest and ozone concentrations affect stratospheric temperatures (McLandress et al., 2010; Thompson et al., 2011).

Recently, the SH stratospheric polar vortex showed an enhanced interannual variability (World Meteorological Organization (WMO), 2022). Although this variability is dynamically driven, it requires a background state which allows for upward wave



60 propagation (Charney and Drazin, 1961). As stated above, GHGs as well as stratospheric ozone can impact the mean state of the vortex. While the observed increase in GHGs is ongoing, a leveling off in the ozone trend was observed in the beginning of the 21st century and first signs of a recovery were detected (Solomon et al., 2016). Hence, in the last two decades GHG and ozone trends did not have complementary effects on the stratospheric temperature anymore. Within this period, the two SSWs of 2002 and 2019 occurred. Both events had an impact on the surface climate that resembled characteristics of the negative
65 phase of the tropospheric SAM (Charlton et al., 2005; Lim et al., 2021). The 2019 event contributed to the extensive heat and drought in Australia in the summer of 2019 that culminated in unprecedented wild fires in the southeast of the continent (Lim et al., 2021).

Under future conditions, the competing effect between ozone recovery and GHG increase on the strength of the stratospheric polar vortex will become stronger and will have a significant impact on the evolution of the SAM in the stratosphere and
70 the troposphere during late spring and summer (Thompson and Solomon, 2005). These opposing effects and uncertainties, connected to future GHG concentrations, the rate of ozone recovery (or the onset of super recovery) and the role of the interaction between GHGs and ozone, lead to uncertainties in the mean state and the variability of the stratospheric polar vortex under future climate conditions (Hawkins and Sutton, 2009; Eyring et al., 2010; Morgenstern et al., 2014; Ivanciu et al., 2022a). This will in turn affect the probability of extreme events in the stratosphere, such as SSWs.

75 The knowledge we have on SH SSWs under historical atmospheric conditions in the SH is restricted to only two events. How frequent SH SSWs are is therefore a question that can only roughly be estimated from observations. Considering that the data availability allows for an identification of SSWs for a maximum period of 67 years (from 1957 to 2023, Naujokat and Roscoe, 2005), a frequency of one major (minor) event per 67 (33.5) years can be estimated. Model simulations show a slightly higher frequency: Wang et al. (2020) found one major SSW every 2-3 decades in a large ensemble of the Met Office GloSea5 seasonal
80 forecasting system, which is based on the high resolution version of the Hadley Centre Global Environment Model version 3 (HadGEM3), whereas Jucker et al. (2021) found one major (minor) SSW every 59 (22) years using a multi-millennial simulation of the Geophysical Fluid Dynamics Laboratory Coupled Model-2.1 (GFDL-CM2.1) under 1990 conditions. The estimate by Jucker et al. (2021) is very close to that estimated from observations. Under future climate conditions (4xCO₂ experiment), Jucker et al. (2021) found a significant decrease in SSW occurrence: one major (minor) SSW every 883 (309)
85 years. They attributed this strong decrease in frequency to the strengthening and to the lifetime extension of the stratospheric polar vortex. They concluded that the 2019 event might be the last one observed in this century. However, this result was based on an extreme, 4xCO₂, GHG forcing setup. Changes in ozone, on the other hand, were not considered, likely resulting in an overestimation of the strengthening of the polar vortex by the end of the century. Further, climate will only see a gradual increase in GHGs as well an increase in ozone in the next decades.

90 The main objective of our study is to evaluate how frequency, timing and coupling characteristics of SH SSWs evolve under various intermediate and strong global warming conditions. In order to address this, we performed time slice simulations with a global atmosphere model under different global warming levels (present-day, 1.5 K, 2 K, 3 K and 4 K). To validate that the model is fit for purpose, we additionally performed an ensemble of historical simulations. The time slice simulations enable us to characterize the development of SSW occurrence for strong as well as for moderate warming levels that we might observe in



95 the coming decades (Intergovernmental Panel on Climate Change (IPCC), 2023). To investigate changes in the surface impacts of SH SSWs we apply a method to distinguish downward propagating and non-propagating SSWs based on the definition by Karpechko et al. (2017), which was created for the NH. Here, we show that this method can also be applied for the SH. Given the large impact that the 2019 SSW had on Australian climate, we think it is important to close the existing knowledge gap and understand the behavior of SH SSWs under different warming levels better.

100 2 Data and Methods

2.1 Model Simulations

We performed model experiments with the Flexible Ocean and Climate Infrastructure, version 1 (FOCI1, Matthes et al., 2020) in the following setting: atmosphere and land model are coupled while SSTs and SIC are prescribed as daily mean values. FOCI1 incorporates the atmosphere model ECHAM, version 6.3.05p2, with a spectral truncation of T63 (about $\sim 1.8^\circ$ in
105 longitude and latitude) and 95 hybrid sigma-pressure levels in the vertical with a lid at 0.01 hPa (Müller et al., 2019) resulting in a realistic representation of important stratospheric features such as the quasi-biennial oscillation or the SSW frequency in the northern hemisphere (Matthes et al., 2020). It also includes the land model: Jena Scheme for Biosphere-Atmosphere Coupling in Hamburg (JSBACH), version 3 (Brovkin et al., 2009; Reick et al., 2013). In our model settings, the dynamical vegetation is not used; vegetation and land use maps are prescribed based on CMIP6 forcing fields. This assures to have the
110 same vegetation cover in each of the model years in the respective time slice experiments.

To analyze the effect of SH SSWs on the surface climate under different global warming levels we performed ensembles of 2 to 3 time slice experiments with about 100 years each for different global warming states: present-day, 1.5 K, 2 K, 3 K and 4 K global warming levels with respect to pre-industrial temperatures. Additionally we performed an ensemble of 5 transient simulations under historical conditions for the period of 1980 to 2019 and compare those to ERA5 data, the latest reanalysis
115 product from the European Centre for Medium-Range Weather Forecasts (ECMWF) (Hersbach et al., 2020), of the same time period. All model experiments are summarized in Table 1. For the historical, as well as for the 2018 experiment, SSTs and SIC are prescribed based on ERA5 data. All external and internal forcing parameters are based on the CMIP6 historical forcing until 2014 and the SSP5-8.5 scenario thereafter (Meinshausen et al., 2020).

The time slice experiments apply perpetual atmospheric and surface conditions that follow the given global warming levels.
120 For the present-day experiment, these conditions follow the 2018 values from the SSP5-8.5 scenario. To calculate the external forcings and boundary conditions for the other warming levels, we used a coupled FOCI1 simulation under the SSP5-8.5 scenario. The respective model years in which the individual warming levels are reached were determined, and a period of ± 15 years for 1.5, 2 and 3 K (± 10 years for 4 K) was used to calculate GHG, stratospheric ozone, solar, aerosol and landuse forcing conditions for the respective global warming experiments. To design the SST and SIC forcing, SST trends from 2018
125 to the 1.5, 2, 3 and 4 K warming level periods from the FOCI1 simulation under the SSP5-8.5 scenario were added to the daily 2018 SST field that was used for the present day experiment up to 60° latitude. Poleward of 60° SST and SIC smoothly transition towards the simulated SIC and SSTs from the FOCI1 simulation under the SSP5-8.5 scenario. This ensures a daily



130 evolution of SST and SIC in each scenario, and minimizes the impact of biases of FOCI1 equatorward of 60°. For all time slice experiments, 20 days at the beginning and end of the respective forcing years were tapered for a smooth transition between the model years.

Table 1. Overview of SSW types and their frequency in ERA5 data and model experiments. In brackets the numbers of dSSWs and nSSWs are indicated (dSSWs/nSSWs).

Experiment	Runs	Years	Forcing type	All SSWs	Majors SSWs	Minor SSWs	1 SSW per	1 major SSW per
ERA5	-	40	-	2 (1/1)	1 (0/1)	1 (1/0)	20 years	40 years
historical	5	200	transient 1980 to 2019	17 (13/4)	7 (6/1)	10 (7/3)	12 years	29 years
present day	3	302	perpetual 2018 conditions	31 (26/5)	7 (7/0)	24 (19/5)	10 years	43 years
1.5K	2	203	perpetual 1.5 K warming	18 (15/3)	7 (7/0)	11 (8/3)	11 years	29 years
2K	2	204	perpetual 2 K warming	19 (10/9)	4 (4/0)	15 (6/9)	11 years	51 years
3K	2	203	perpetual 3 K warming	12 (9/3)	2 (2/0)	10 (7/3)	17 years	102 years
4K	2	201	perpetual 4 K warming	14 (9/5)	1 (1/0)	13 (8/5)	14 years	201 years

2.2 Methods

We define major and minor SSW events for the SH. In the first case, we follow the definition for the NH (Charlton and Polvani, 2007), for which major SSW events are defined when the zonal mean zonal wind at 60°latitude and 10 hPa (U_{1060}) turns easterly during winter or early spring and recovers to westerlies for at least 10 consecutive days before the end of April. For the SH we select the period from July to September for the detection of major SSWs. The central date (or day 0) of a major SSW is defined as the first day when this criterion is met. To distinguish an SSW from an early final warming, the zonal mean zonal wind has to return to westerlies for at least 10 consecutive days prior to the final breakdown of the polar stratospheric vortex. For minor warmings we use a threshold of 20 m/s as done in Rao et al. (2022) and follow the definition of major SSWs in all other aspects. This method captures the observed stratospheric warmings in the SH when applied to ERA5 data and is therefore regarded to be suitable for our analysis (compare Fig. 1). For parts of the analysis we combine major and minor events and refer to these as "all SSWs".

145 Additionally, we applied a method to investigate whether an SSW signal propagates into the troposphere by distinguishing between downward propagating and non-propagating SSWs based on the definition introduced by Karpechko et al. (2017) for the NH, that uses the Norther Annular Mode. Here, we use the Southern Annular Mode (SAM, defined below) and follow three criteria (Karpechko et al., 2017):

- (1) The mean SAM index at 1000 hPa (SAM1000) over the period of 45 days (days 8-52 after day 0) must be negative
- (2) the proportion of days within this 45-day period on which the daily SAM1000 is negative shall be at least 50%



- (3) the proportion of days within that 45-day period on which the daily SAM indices in the lower stratosphere (SAM150) are negative shall be at least 70%

- 150 The SAM is defined analogous to a simple approach used for the Northern Annular Mode in Karpechko et al. (2017): geopotential height (GPH) is averaged over the polar cap (60-90°S) after the values are area-weighted. The daily climatology is subtracted to calculate the respective anomalies for each pressure level. After that, the data in each level is normalized by its standard deviation. Conventionally, the SAM is defined as negative if the polar cap GPH anomalies are positive. To achieve this, the SAM index is multiplied by minus 1 for each pressure level.
- 155 For the surface responses to SSWs as well as for the SSW downward propagation signal in the SAM, composite analysis is applied. For the SAM, composites are calculated with respect to the central day of the SSW events. For the surface response, the anomaly of the October to December period for SSW years is used, which is similar to the definition used in Lim et al. (2019), who considered the period of October to January in their analyses. Significant differences of these composites to the mean state are calculated based on a two-sided t-test when applicable. Statistical significance is indicated for p-values ≤ 0.05 .

160

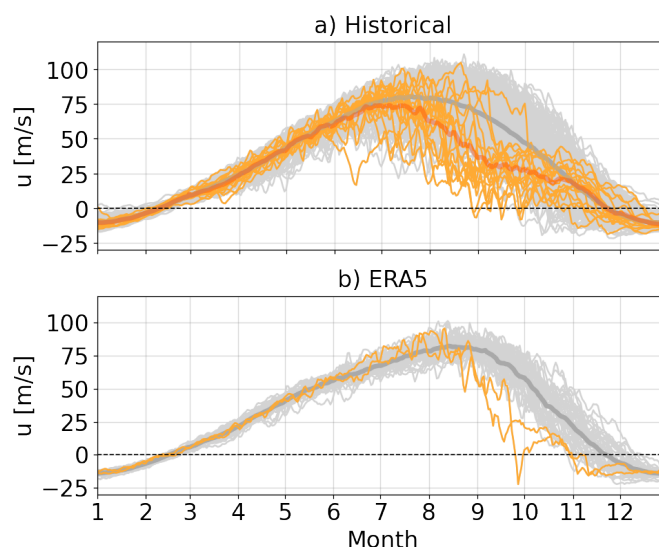


Figure 1. Annual cycle of zonal mean zonal wind (U) at 10 hPa and 60°S of individual years (thin gray lines) and the multi-year mean (thick gray line) for a) the historical model ensemble and b) ERA5 data. Thin orange lines indicate years for which a stratospheric warming event was found. The thick orange line shows the mean of all SSW years. The dashed line highlights the zero wind line. The ticks on the x-axis indicate the start of the months.



3 Results: SSWs in FOCI1 and its effect on Australian heat events

3.1 SH SSWs under historical and present-day conditions

Before we investigate the impact of climate change on the frequency and surface impacts of stratospheric warmings, we want to show how well FOCI1 represents SH SSWs and their impact onto the surface under historical and present-day conditions. Figure 1 shows the zonal mean zonal wind at 10 hPa and 60 °S for the historical ensemble (Fig. 1a) and for ERA5 (Fig. 1b). The multiyear mean (thick gray line) shows that the maximum wind in FOCI1 is reached earlier than in ERA5 but that it is of comparable magnitude. In contrast to the reanalysis data, our historical ensemble shows a larger spread among modeled years, reflecting a higher interannual variability in the strength of the polar vortex in comparison to ERA5. The colored lines show those years that classify as years with a minor or major warming according to the definitions given above. Our definition clearly captures the observed warming years, 2002 and 2019 in ERA5 (Fig. 1b). The frequency of SSWs in the historical ensemble is almost twice as high as in ERA5 (Table 1). However, the occurrence of SSWs for single ensemble members ranges from 0 to 7 events in the 40-year period from 1980 to 2019. The number of observed SSWs falls within this spread.

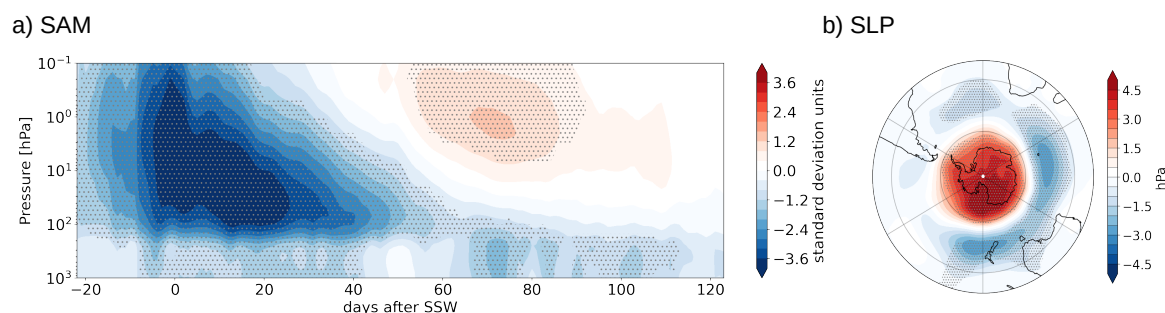


Figure 2. SSW composites for the historical ensemble of a) Southern Annular Mode (SAM) anomalies relative to the central day (day 0) and of (b) SLP anomalies averaged over October, November and December in SSW years / following an SSW. Areas that show significant anomalies with respect to the climatology based on a two-sided t-test are stippled ($p\text{-value} \leq 0.05$).

To evaluate FOCI's representation of the impact of SH SSWs on the troposphere, we will focus on the SSW related anomalies of the SAM next. The temporal evolution of SAM anomalies throughout the middle and lower atmosphere following the defined SSW events is depicted in Figure 2a. Minor and major warmings are considered together in this figure. The central day is defined as the first day for which U_{1060} drops below 20 m/s for major and minor warmings. The negative stratospheric SAM anomaly associated with an SSW event sets in already before the criterion for the SSW is met. It propagates downward within the stratosphere after the central day and persists in a large region of the lower stratosphere for up to 60 days after the SSW onset. The tropospheric SAM is negative from about 5 days before the central day and stays negative for more than 100 days. This persistent SAM anomaly has influences onto the surface climate. Figure 2b shows the SLP anomaly during SSW summers. It shows a clear annular mode signature with high pressure anomalies over Antarctica and a low pressure anomaly band between

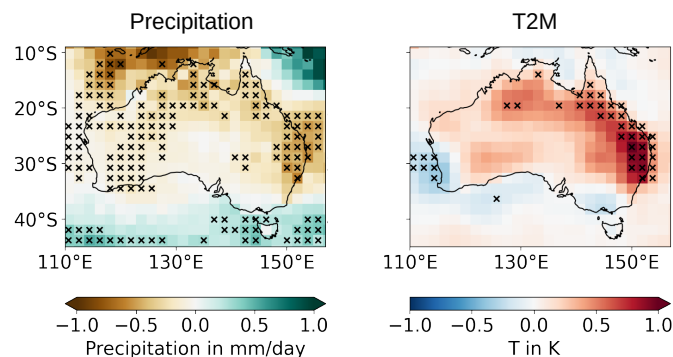


Figure 3. SSW composite for the historical ensemble of anomalies in precipitation (left) and 2m air temperature (right). Anomalies are averaged over the October-November-December period for years with an SSW. Significance with respect to the climatology is indicated by stippling ($p - value \leq 0.05$).

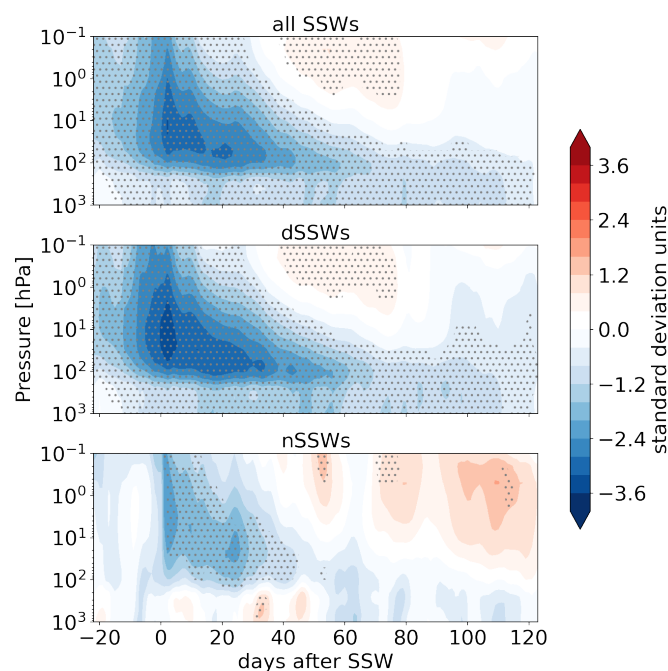


Figure 4. Composite of Southern Annular Mode anomalies relative to the central day (day 0) of different SSW events for the present-day experiment: (top to bottom) all SSWs, downward propagating SSWs (dSSWs) and non-propagating SSWs (nSSWs). Areas that show significant SAM anomalies with respect to the climatology based on a two-sided t-test are stippled ($p - value \leq 0.05$).

30 to 50°S. However, the low SLP anomaly band is not completely symmetric around the pole. Largest anomalies are found in the Indian and West-Pacific sectors of the Southern Ocean, impacting especially the Australian continent where we find significant anomalies in precipitation and 2m air temperature (T2M) during SSW summers (Fig. 3). These are dominated by

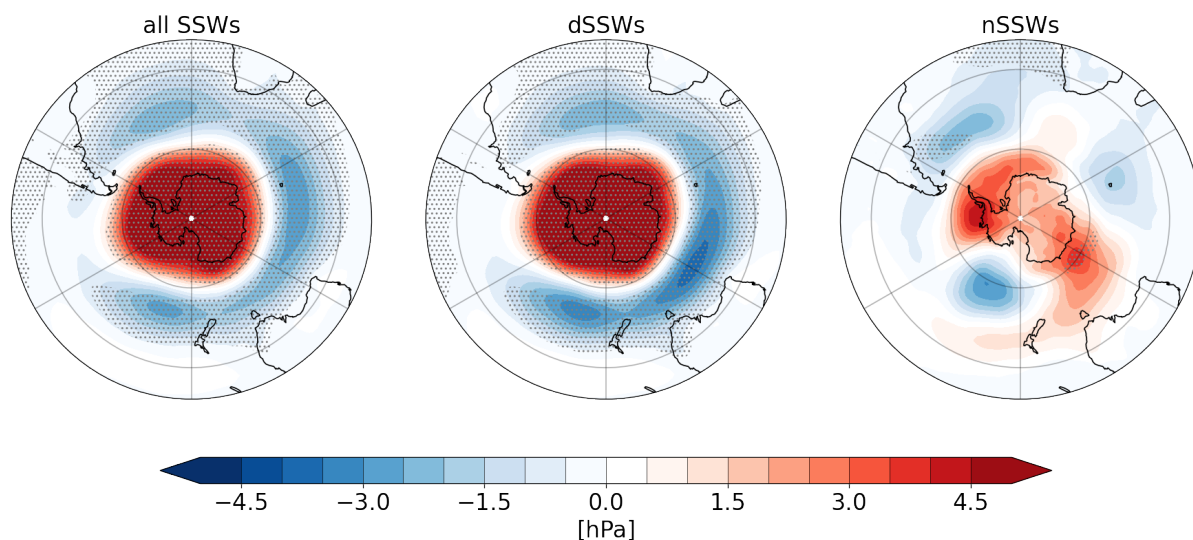


Figure 5. Composite of SLP anomalies for the present-day experiment averaged over OND for (left to right) years with SSWs, years with downward propagating SSWs (dSSWs) and years with non-propagating SSWs (nSSWs). Stippling indicates significance ($p\text{-value} \leq 0.05$)

precipitation deficiencies over large parts of Australia and enhanced air temperatures over the north-eastern part of the country. This response compares very well to the findings by Lim et al. (2019) and Lim et al. (2021).

In order to address the evolution of SSWs under global warming conditions, time slice experiments under different global warming levels were conducted. To ensure that this model setup compares well to the historical ensemble run under transient conditions, we ran a time-slice simulation under present-day (perpetual 2018) conditions, which we want to consider first. Table 1 shows that the frequency of SSWs in this experimental setup is close to the historical ensemble (1 SSW every 12 years and every 10 years respectively). The downward propagation of the SAM anomalies (Fig. 4a), as well as the surface response in SLP (Fig. 5a), temperature and precipitation (Fig. 6a) compare very well to our results from the historical ensemble. The largest difference in the response is found in western Australia, where the present-day experiment lacks the deficit in precipitation but shows a significant increase in air temperature in comparison to the historical ensemble. However, with these differences, the response of the present-day experiment fits the observed response as described by Lim et al. (2019) even better than our historical setup did. We will therefore use this time slice setup for further analyses.

3.2 Downward coupling of SH SSWs

To test how stratosphere-troposphere coupling changes under global warming, we distinguish between downward propagating SSWs (dSSWs) and non-propagating SSWs (nSSWs). The numbers of dSSWs and nSSWs in the different experiments are shown in Table 1 in brackets. While almost all major warmings classify as dSSWs, minor warmings can classify as both types. The atmospheric responses to dSSW and nSSW events for the present-day experiment are shown in Figures 4-6b and 4-6c,

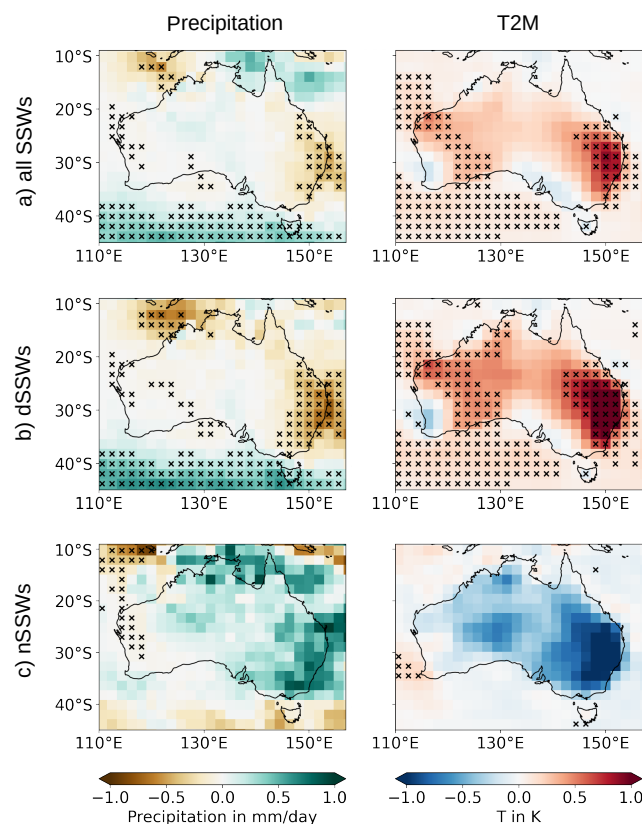


Figure 6. SSW composite for the present-day experiment of anomalies in precipitation (left) and 2m air temperature (right) for a) all SSWs, b) downward propagating SSWs (dSSWs) and c) non-propagating SSWs (nSSWs). Anomalies are averaged over the October–November–December period for years with respective SSW events. Significance is indicated by stippling ($p - value \leq 0.05$).

Table 2. Number of dSSWs and nSSWs per decade under different global warming levels.

Experiment	dSSWs/decade	nSSWs/decade
historical	0.65	0.20
present day	0.86	0.17
1.5K	0.74	0.15
2K	0.49	0.44
3K	0.44	0.15
4K	0.45	0.25

respectively. It becomes clear that the method, which was introduced by Karpechko et al. (2017) for the NH, also fits very well for the SH. In winters with dSSWs a clear SAM-like response is found in the atmosphere. Further, dSSWs dominate the

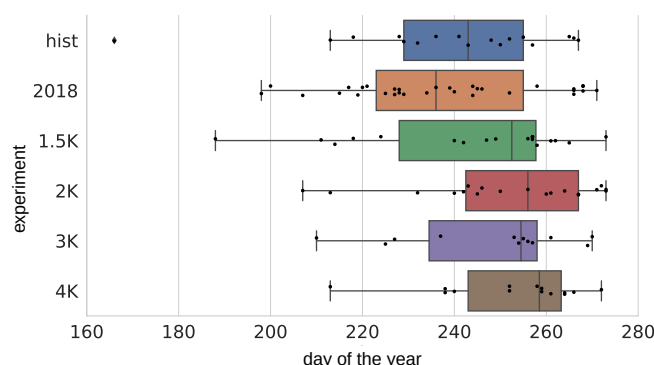


Figure 7. Boxplot of SSW onset days. Different colors denote the different model experiments. Black dots show the individual events that were considered for the statistics, while diamonds show outliers. The box represents the quartiles, the whiskers the spread of the distribution (excluding outliers). The median is indicated by a solid line.

composites when considering all SSWs. The tropospheric SAM does not show any significant negative anomalies after nSSWs (Fig. 4c), which is in line with the surface SLP response to nSSWs missing the typical annular mode like structure (Fig. 5c) and with the missing surface response in temperature and precipitation over the Australian continent (Fig. 6c). The lack of negative SAM anomalies during nSSWs as well as the insignificant surface responses imply that the stratosphere does not influence the troposphere after nSSWs. Hence, the comparison between dSSW and nSSW occurrence shall give valuable information on the strength of the stratosphere-troposphere coupling between the different simulations.

Table 2 shows the frequency of dSSWs and nSSWs per decade for all the model experiments we conducted. Comparing the historical to the present-day experiments shows that dSSWs are more frequent under present-day conditions (0.65 dSSW/decade vs. 0.86 dSSWs/decade), while the frequency of nSSWs is very similar between both experiments (0.20 nSSWs/decade vs. 0.17 nSSWs/decade).

3.3 Global warming conditions

Under global warming conditions, our experiments show a decrease in the frequency of dSSWs from 0.65-0.86 dSSW/decade under historical and present-day conditions to about 0.45 dSSWs/decade for a warming of 3 to 4 K (Table 2). The frequency of nSSWs does not decrease linearly with global warming; it stays between 0.15 and 0.25 nSSWs/decade, with the exception of the 2 K experiment, in which we find a higher frequency of nSSWs (0.44 nSSWs/decade). Overall, the ratio between dSSWs and nSSWs indicates that the coupling between the stratosphere and the troposphere decreases under increasing levels of global warming, although not linearly.

Figure 7 shows the distribution of SSW onset days among the different experiments. While the median of the distribution is close to day 240 for the historical and the present-day experiments, it shifts towards later onset dates starting already at a warming of 1.5K. Late warmings are frequent especially for the 2K warming experiment. Distinguishing between dSSW and nSSW onset days indicates that dSSWs tend to occur earlier in the season than nSSWs in the time slice experiments under

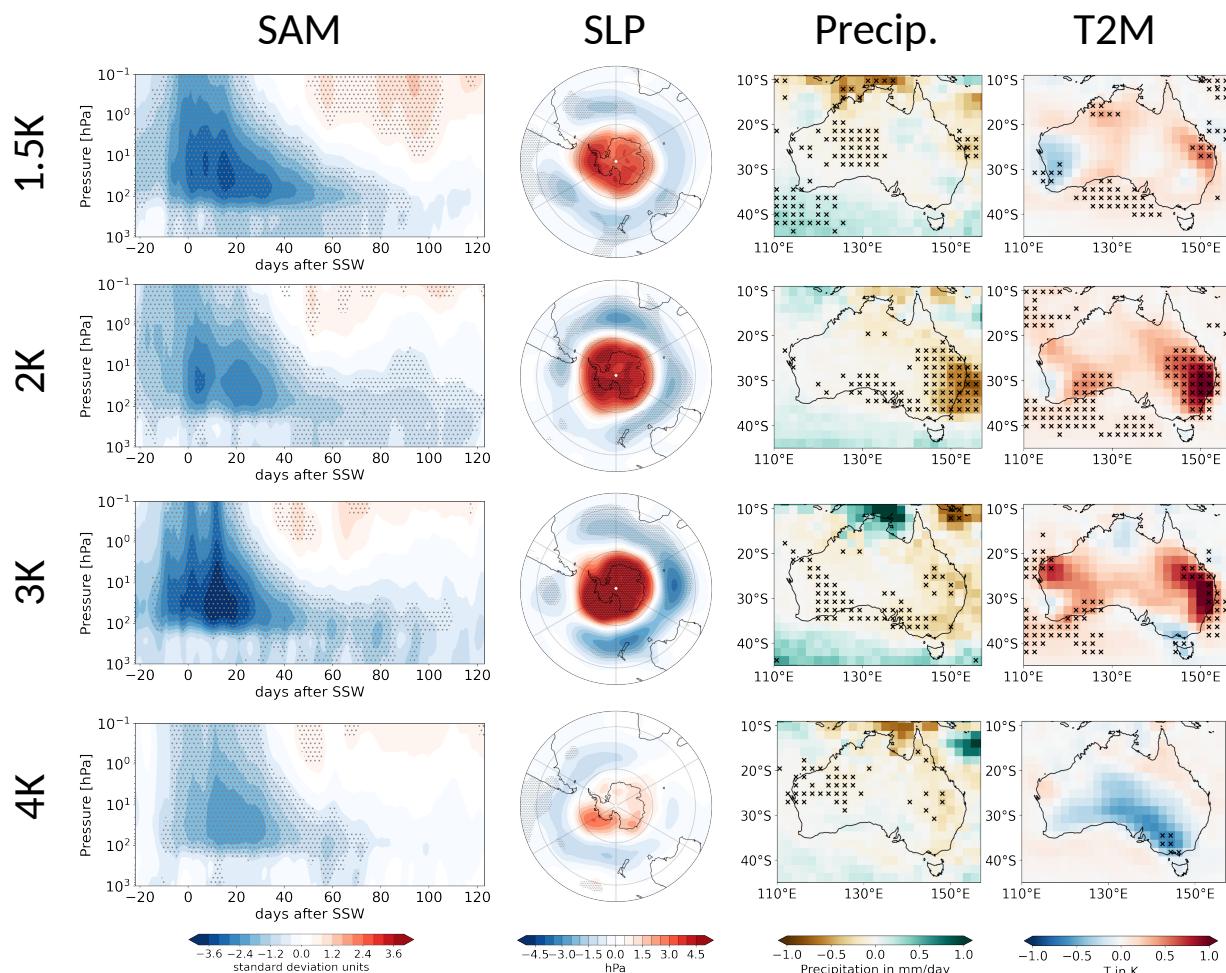


Figure 8. SSW composites for the different global warming levels: 1.5 K, 2 K, 3 K, and 4 K (top to bottom) showing anomalies of the SAM with respect to the central day of the SSWs, as well as of SLP, precipitation (Precip.) and 2 m air temperature (T2M) averaged over OND for years with SSWs (left to right). Stippling indicates statistical significance ($p - value \leq 0.05$).

present-day, 1.5K and 2K conditions (Supplementary Fig. S1). This relation, however, might be influenced by the small number of nSSWs in comparison to dSSWs and should be interpreted with caution.

The decrease in dSSWs with global warming (Table 2) generally leads to a decrease in the strength of the coupling between the stratosphere and the troposphere. This response is not linearly reflected in the SAM and surface anomalies (Fig. 8). While the number of nSSWs is very high in the 2K experiment, the downward propagating events are exceptionally strong and long-lasting and dominate the composites with strong signals in precipitation and temperature anomalies over Australia (Supplementary Figs. S2 and S3). On the other hand, for the 1.5K warming ensemble, the surface response is relatively weak compared to the historical, present-day, 2K and 3K warming experiments (compare Figs. 3, 6, and 8).

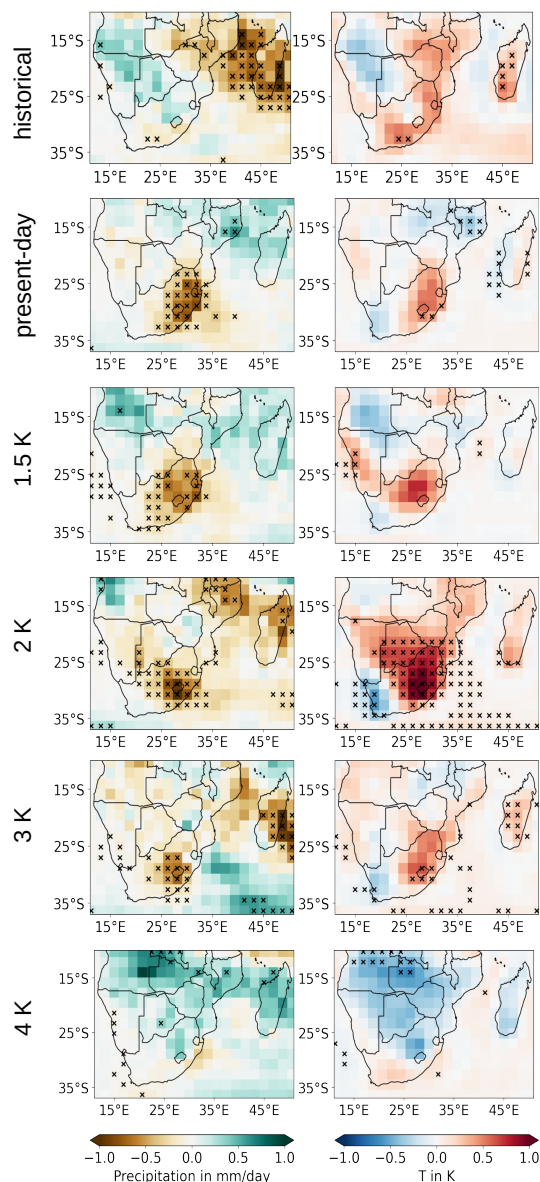


Figure 9. SSW composites for South Africa in all model experiments: historical, present-day, 1.5K, 2K, 3K, and 4K (top to bottom) showing anomalies in precipitation (left column) and 2 m air temperature (right column) averaged over OND for years with SSWs. Stippling indicates statistical significance ($p - value \leq 0.05$).

235 A clear cut in the SAM and surface responses to SSWs occurs only under 4K conditions. In this experiment the SLP response is insignificant and also the precipitation and temperature signals over Australia differ remarkably from the response under present-day and historical conditions (Fig. 8, bottom row corresponding to 4 K warming level). However, when considering



only dSSWs (Supplementary Fig. S2) the typical precipitation response over eastern Australia is also apparent for a 4K warmer world, the T2M response stays insignificant.

240 Another region that is significantly impacted by SH SSWs is South Africa. Figure 9 shows the surface response to SSWs in precipitation and 2 m air temperature over the southern tip of the African continent for all of the model experiments. Under historical and present-day conditions, the temperature response shows a tendency for warmer than normal conditions in the south east of the continent. However, this signal is only marginally significant. The precipitation response, which can be described by drier than normal conditions, dominates over Mozambique and Madagascar for the historical ensemble and over the
245 country of South Africa in the present-day simulation.

The global warming time slice experiments agree on the deficiency in precipitation over this southern most region of the continent up to a warming of 3K. The temperature response is of less statistical significance with the exception of the 2K experiment. Here, a significant warming over large parts of South Africa and Botswana and a significant cooling over the western tip of South Africa can be identified. This experiment also showed the strongest signal over Australia (Fig. 8). For a warming of
250 4K, no significant response to SSWs can be found. This is in agreement with the previously described reduction in STC in this experiment. These surface responses to SSWs over the South African continent are consistent with the response to dSSWs only (Supplementary Fig. S4).

We do not find such a robust SSW response in precipitation and air temperature over New Zealand and South America among the different experiments (Supplementary Figs. S5 and S6). However, our simulations are indicative of a tendency for wetter
255 and colder conditions over southern South America and New Zealand after SH SSWs.

To analyze why the SSW frequency changes with global warming, we consider the change in the zonal mean zonal wind at 10 hPa between 55 to 65°S and the polar cap temperature (south of 60°S) at 30 hPa (Fig. 10). Figures 10a and b show the climatologies for the different time slice experiments, while Fig. 10c and d show the differences of the warming experiments to the present-day experiment (blue line). As expected, the lower stratosphere gets colder throughout the year under increasing
260 levels of global warming. This also leads to an increase in strength of the stratospheric polar vortex throughout most of its lifetime. These changes, however, are not only dependent on the GHG concentrations that drive the level of global warming, but also on the recovery of ozone (Supplementary Fig. S7), whose effect is most pronounced in austral spring. In fact, most of the global warming experiments show a decrease in the strength of the westerly winds between 55 to 65°S at 10 hPa during that time of the year (between days 270 and 340). The change in the strength of the westerly wind with respect to the present-day
265 experiment is remarkably similar for the warming levels of 1.5, 2 and 3 K during this time of year. Also the 4K experiment shows this weakening of the westerly winds later in the year, i.e. at the end of the polar vortex lifetime.

Considering the temperature response, all but the 4K experiment show polar cap temperatures that are similar to present-day conditions or higher in spring peaking around day 300. This indicates that the interplay between GHG increase and ozone recovery plays a key role in the strength of the vortex (in agreement with McLandress et al., 2010). It is the period between
270 days 250 and 260 (beginning of September) in which most of the SSWs occur in the global warming experiments (Fig. 7). This is the period, when zonal winds are closest to the present-day conditions in the 1.5, 2 and 3K global warming experiments (Fig.



10).

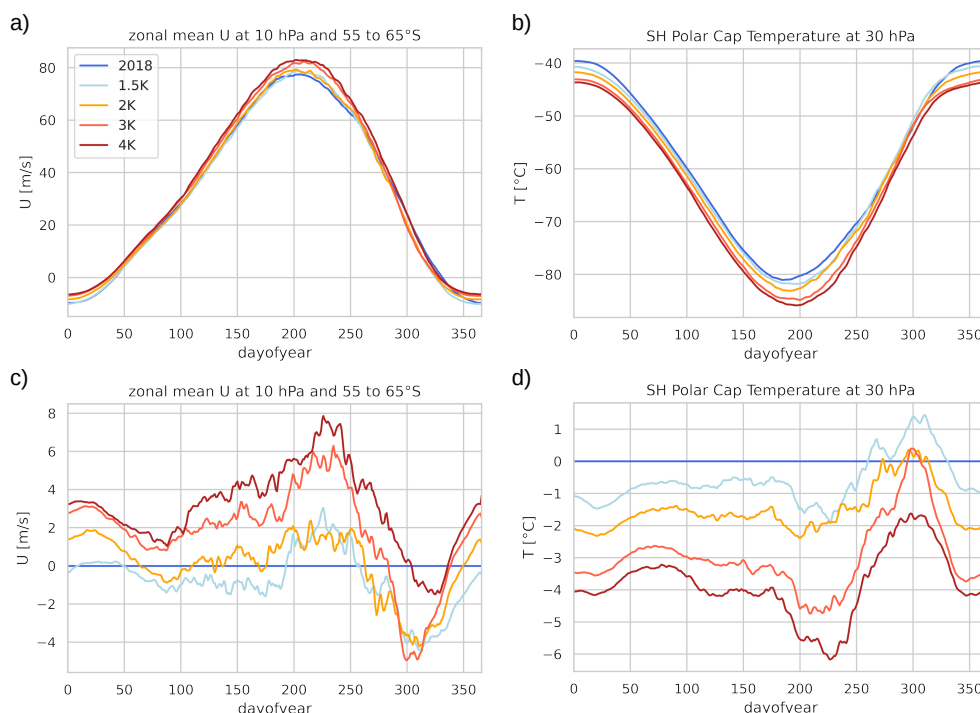


Figure 10. Seasonal cycle of zonal mean zonal wind at 10 hPa and 55 to 65°S (a) and polar cap temperatures at 30 hPa (b) for the different time slice experiments: 2018 (present-day, dark blue), 1.5 K (light blue), 2 K (yellow), 3 K (orange), and 4 K (red). (c) and (d) as in (a) and (b) but as the anomaly between the different global warming experiments to the present-day experiment.

4 Conclusion

275 In this paper we investigated the frequency of SH SSWs, the change in coupling strength between the stratosphere and troposphere for these events under different global warming levels (present-day, 1.5 K, 2 K, 3 K and 4 K) and the associated changes in surface responses to SH SSWs.

As expected, we find a decrease in the frequency of SSWs under global warming. The strongest decrease is found for the number of major SSWs from about 1 major SSW in 30 to 40 years under present-day conditions to 1 major SSW in 200 years
280 under a global warming of 4 K. Considering dSSWs, we find a decrease from 0.65-0.86 dSSW/decade under historical and present-day conditions to about 0.45 dSSWs/decade for the warming levels of 3 to 4 K (Tables 1 and 2).

Our FOCI1 experiments simulate the expected response to SSWs over Australia as presented in Lim et al. (2019) under historical and present-day conditions with positive temperature and negative precipitation anomalies during summer over eastern



Australia in SSW years (see section 3.1). We found that this response is also expected for global warming levels of up to 3 K, while no significant surface response was found for a warming of 4 K.

In comparison to the study by Jucker et al. (2021) the frequency of SSWs is higher in our FOCI1 simulations under present-day conditions: 1 SSW every 10 years in our simulation and 1 SSW every 22 years in Jucker et al. (2021). Furthermore, while Jucker et al. (2021) find a strong decrease in SSW frequency under high GHG forcing (1 event every 309 years), the frequency in our simulations decreases only slightly (to 1 event every 14 to 17 years, see Table 1). This difference can at least partly be attributed to a different experimental design. In contrast to Jucker et al. (2021) we prescribe SSTs and SICs, and consider a stratospheric ozone recovery together with the GHG increase. Additionally, we investigated intermediate warming levels to assess SH SSW characteristics, which still have a possibility to occur in the coming decades. Jucker et al. (2021), on the other hand, focused on an end-of-the-century increase in atmospheric CO_2 concentrations in comparison to a perpetual 1990 simulation; their absolute difference in CO_2 concentrations is overall larger than in our present-day vs. 4K experiment.

In this study, we showed that the timing of a decrease in SSW frequency depends on the interplay between GHG increase and ozone recovery. Ozone recovery is of particular importance since it is of largest amplitude in September when most SSWs occur. Our findings imply that SSWs on the SH can still occur under climate change conditions despite the ongoing increase in GHG concentrations. Given that the CMIP6 ozone recovery used in our study is weaker than chemistry climate models suggest (Ivanciu et al., 2022b), the actual impact of ozone recovery might be even larger than suggested by our simulations. Our simulations also miss the interaction between ozone and stratospheric dynamics, which was shown to enhance anomalies within the stratosphere and thereby also the tropospheric response to these anomalies (Haase et al., 2020). In the medium-range ECMWF forecasting system, improvements in the response of high-latitude tropospheric winds to the 2002 SSW event were found when including a new stratospheric ozone model which significantly improved the representation of the SH stratospheric polar vortex including its seasonality (Monge-Sanz et al., 2022). Particularly, for the 2002 major SSW, Hendon et al. (2020) showed that the stratospheric SAM anomaly and the associated surface responses over Australia connected to this warming were enhanced by positive ozone feedbacks.

Despite missing chemistry-climate feedbacks in our model setup, the prescribed recovery of the ozone layer counteracts the GHG-driven strengthening of the polar stratospheric vortex in such a way that the frequency of SSWs remains nearly unchanged up to a warming of 2 K. This suggests that SH SSWs and their impacts on weather conditions in Australia and Southern Africa, as shown in Figures 8 and 9, will still be significant in the coming decades. Therefore, it is crucial not to overlook SH SSWs as an influential factor in extreme weather forecasting for these regions in the near future.

Data availability. ERA5 data (Hersbach et al., 2020) is available via the Copernicus Climate Data Store (<https://cds.climate.copernicus.eu>). The model data used in this manuscript is published (Bischof et al., 2025) and available via <https://zenodo.org/doi/10.5281/zenodo.16876611>.



315 *Author contributions.* This study is partly based on the Bachelor Thesis by PH (Garden, 2022); SB wrote the manuscript and contributed substantially to the methodology design, data analysis and figure refinements; PR did large parts of the analysis and figures; RPK initiated the study, designed the methodology and guided its development; WH contributed to the design of the methodology; SW, RPK and SB designed and ran the model simulations; all authors contributed with discussions and feedback on the paper draft.

Competing interests. The authors declare that no competing interests are present.

320 *Acknowledgements.* This study was mainly funded by the GEOMAR Helmholtz Centre for Ocean Research in Kiel. Part of the funding for SB and RPK was granted through the ‘Drivers of Jet stream anomalies’ project of the Helmholtz Initiative on Climate Adaptation and Mitigation (HI-CAM) under the grant number RA-285/19. The model simulations were performed with resources provided by the North-German Supercomputing Alliance (HLRN), project shk00018.



References

- Baldwin, M. P. and Dunkerton, T. J.: Stratospheric harbingers of anomalous weather regimes, *Science* (New York, N.Y.), 294, 581–4, <https://doi.org/10.1126/science.1063315>, 2001.
- Bischof, S., Pilch Kedzierski, R., and Wahl, S.: Bischof et al. 2025 - Southern Hemisphere Sudden Stratospheric Warmings Continue to Be Relevant Under Global Warming, [Data set], <https://doi.org/10.5281/ZENODO.16876611>, 2025.
- Brovkin, V., Raddatz, T., Reick, C. H., Claussen, M., and Gayler, V.: Global biogeophysical interactions between forest and climate, *Geophysical Research Letters*, 36, 1–5, <https://doi.org/10.1029/2009GL037543>, 2009.
- Butler, A. H., Seidel, D. J., Hardiman, S. C., Butchart, N., Birner, T., and Match, A.: Defining Sudden Stratospheric Warmings, *Bulletin of the American Meteorological Society*, 96, 1913–1928, <https://doi.org/10.1175/BAMS-D-13-00173.1>, 2015.
- Butler, A. H., Sjöberg, J. P., Seidel, D. J., and Rosenlof, K. H.: A sudden stratospheric warming compendium, *Earth System Science Data*, 9, 63–76, <https://doi.org/10.5194/essd-9-63-2017>, 2017.
- Charlton, A. J. and Polvani, L. M.: A New Look at Stratospheric Sudden Warmings. Part I: Climatology and Modeling Benchmarks, *Journal of Climate*, 20, 449–469, <https://doi.org/10.1175/JCLI3996.1>, 2007.
- Charlton, A. J., O'Neill, A., Lahoz, W. A., Massacand, A. C., and Berrisford, P.: The impact of the stratosphere on the troposphere during the southern hemisphere stratospheric sudden warming, September 2002, *Quarterly Journal of the Royal Meteorological Society*, 131, 2171–2188, <https://doi.org/10.1256/qj.04.43>, 2005.
- Charney, J. G. and Drazin, P. G.: Propagation of planetary-scale disturbances from the lower into the upper atmosphere, *Journal of Geophysical Research*, 66, 83–109, <https://doi.org/10.1029/JZ066i001p00083>, 1961.
- Dennison, F. W., McDonald, A. J., and Morgenstern, O.: The effect of ozone depletion on the Southern Annular Mode and stratosphere-troposphere coupling, *Journal of Geophysical Research Atmospheres*, 120, 1–8, <https://doi.org/10.1002/2014JD023009>, 2015.
- Eyring, V., Cionni, I., Bodeker, G. E., Charlton-Perez, A. J., Kinnison, D. E., Scinocca, J. F., Waugh, D. W., Akiyoshi, H., Bekki, S., Chipperfield, M. P., Dameris, M., Dhomse, S., Frith, S. M., Garny, H., Gettelman, A., Kubin, A., Langematz, U., Mancini, E., Marchand, M., Nakamura, T., Oman, L. D., Pawson, S., Pitari, G., Plummer, D. a., Rozanov, E., Shepherd, T. G., Shibata, K., Tian, W., Braesicke, P., Hardiman, S. C., Lamarque, J. F., Morgenstern, O., Pyle, J. A., Smale, D., and Yamashita, Y.: Multi-model assessment of stratospheric ozone return dates and ozone recovery in CCMVal-2 models, *Atmospheric Chemistry and Physics*, 10, 9451–9472, <https://doi.org/10.5194/acp-10-9451-2010>, 2010.
- Garden, P. U.: Southern hemisphere sudden stratospheric warmings in the ECHAM6 model, Ph.D. thesis, CAU Kiel, 2022.
- Gillett, N. P. and Thompson, D. W. J.: Simulation of Recent Southern Hemisphere Climate Change, *Science*, 302, 273–275, <https://doi.org/10.1126/science.1087440>, 2003.
- Haase, S., Fricke, J., Kruschke, T., Wahl, S., and Matthes, K.: Sensitivity of the Southern Hemisphere circumpolar jet response to Antarctic ozone depletion: Prescribed versus interactive chemistry, *Atmospheric Chemistry and Physics*, 20, 14043–14061, <https://doi.org/10.5194/acp-20-14043-2020>, 2020.
- Hawkins, E. and Sutton, R.: The Potential to Narrow Uncertainty in Regional Climate Predictions, *Bulletin of the American Meteorological Society*, 90, 1095–1108, <https://doi.org/10.1175/2009BAMS2607.1>, 2009.
- Hendon, H. H., Lim, E. P., and Abhik, S.: Impact of Interannual Ozone Variations on the Downward Coupling of the 2002 Southern Hemisphere Stratospheric Warming, *Journal of Geophysical Research: Atmospheres*, 125, 1–16, <https://doi.org/10.1029/2020JD032952>, 2020.



- Hersbach, H., Bell, B., Berrisford, P., Hirahara, S., Horányi, A., Muñoz-Sabater, J., Nicolas, J., Peubey, C., Radu, R., Schepers, D., Simons, A., Soci, C., Abdalla, S., Abellan, X., Balsamo, G., Bechtold, P., Biavati, G., Bidlot, J., Bonavita, M., De Chiara, G., Dahlgren, P., Dee, D., Diamantakis, M., Dragani, R., Flemming, J., Forbes, R., Fuentes, M., Geer, A., Haimberger, L., Healy, S., Hogan, R. J., Hólm, E., Janisková, M., Keeley, S., Laloyaux, P., Lopez, P., Lupu, C., Radnoti, G., de Rosnay, P., Rozum, I., Vamborg, F., Villaume, S., and Thépaut, J. N.: The ERA5 global reanalysis, *Quarterly Journal of the Royal Meteorological Society*, 146, 1999–2049, <https://doi.org/10.1002/qj.3803>, 2020.
- Intergovernmental Panel on Climate Change (IPCC): Climate Change 2021 – The Physical Science Basis: Working Group I Contribution to the Sixth Assessment Report of the Intergovernmental Panel on Climate Change, Cambridge University Press, Cambridge, United Kingdom and New York, NY, USA, <https://doi.org/10.1017/9781009157896>, 2023.
- Ivanciu, I., Matthes, K., Biastoch, A., Wahl, S., and Harlaß, J.: Twenty-first-century Southern Hemisphere impacts of ozone recovery and climate change from the stratosphere to the ocean, *Weather and Climate Dynamics*, 3, 139–171, <https://doi.org/10.5194/wcd-3-139-2022>, 2022a.
- Ivanciu, I., Ndarana, T., Matthes, K., and Wahl, S.: On the Ridging of the South Atlantic Anticyclone Over South Africa: The Impact of Rossby Wave Breaking and of Climate Change, *Geophysical Research Letters*, 49, <https://doi.org/10.1029/2022GL099607>, 2022b.
- Jucker, M., Reichler, T., and Waugh, D. W.: How Frequent Are Antarctic Sudden Stratospheric Warmings in Present and Future Climate?, *Geophysical Research Letters*, 48, 1–9, <https://doi.org/10.1029/2021GL093215>, 2021.
- Karpechko, A. Y., Hitchcock, P., Peters, D. H. W., and Schneidereit, A.: Predictability of downward propagation of major sudden stratospheric warmings, *Quarterly Journal of the Royal Meteorological Society*, 143, 1459–1470, <https://doi.org/10.1002/qj.3017>, 2017.
- Lim, E. P., Hendon, H. H., Boschat, G., Hudson, D., Thompson, D. W., Dowdy, A. J., and Arblaster, J. M.: Australian hot and dry extremes induced by weakenings of the stratospheric polar vortex, *Nature Geoscience*, 12, 896–901, <https://doi.org/10.1038/s41561-019-0456-x>, 2019.
- Lim, E. P., Hendon, H. H., Butler, A. H., Thompson, D. W., Lawrence, Z. D., Scaife, A. A., Shepherd, T. G., Polichtchouk, I., Nakamura, H., Kobayashi, C., Comer, R., Coy, L., Dowdy, A., Garreaud, R. D., Newman, P. A., and Wang, G.: The 2019 southern hemisphere stratospheric polar vortex weakening and its impacts, *Bulletin of the American Meteorological Society*, 102, E1150–E1171, <https://doi.org/10.1175/BAMS-D-20-0112.1>, 2021.
- Lim, E.-P. P., Hendon, H. H., and Thompson, D. W. J.: Seasonal Evolution of Stratosphere-Troposphere Coupling in the Southern Hemisphere and Implications for the Predictability of Surface Climate, *Journal of Geophysical Research: Atmospheres*, 123, 12,002–12,016, <https://doi.org/10.1029/2018JD029321>, 2018.
- Matthes, K., Biastoch, A., Wahl, S., Harlaß, J., Martin, T., Brücher, T., Drews, A., Ehlert, D., Getzlaff, K., Krüger, F., Rath, W., Scheinert, M., Schwarzkopf, F. U., Bayr, T., Schmidt, H., and Park, W.: The Flexible Ocean and Climate Infrastructure version 1 (FOCI1): mean state and variability, *Geoscientific Model Development*, 13, 2533–2568, <https://doi.org/10.5194/gmd-13-2533-2020>, 2020.
- McLandress, C., Jonsson, A. I., Plummer, D. A., Reader, M. C., Scinocca, J. F., and Shepherd, T. G.: Separating the Dynamical Effects of Climate Change and Ozone Depletion. Part I: Southern Hemisphere Stratosphere, *Journal of Climate*, 23, 5002–5020, <https://doi.org/10.1175/2010JCLI3586.1>, 2010.
- Meinshausen, M., Nicholls, Z. R., Lewis, J., Gidden, M. J., Vogel, E., Freund, M., Beyerle, U., Gessner, C., Nauels, A., Bauer, N., Canadell, J. G., Daniel, J. S., John, A., Krummel, P. B., Luderer, G., Meinshausen, N., Montzka, S. A., Rayner, P. J., Reimann, S., Smith, S. J., Van Den Berg, M., Velders, G. J., Vollmer, M. K., and Wang, R. H.: The shared socio-economic pathway (SSP) greenhouse gas concentrations and their extensions to 2500, *Geoscientific Model Development*, 13, 3571–3605, <https://doi.org/10.5194/gmd-13-3571-2020>, 2020.



- Monge-Sanz, B. M., Bozzo, A., Byrne, N., Chipperfield, M. P., Diamantakis, M., Flemming, J., Gray, L. J., Hogan, R. J., Jones, L., Magnusson, L., Polichtchouk, I., Shepherd, T. G., Wedi, N., and Weisheimer, A.: A stratospheric prognostic ozone for seamless Earth system models: performance, impacts and future, *Atmospheric Chemistry and Physics*, 22, 4277–4302, [https://doi.org/10.5194/acp-22-4277-](https://doi.org/10.5194/acp-22-4277-2022)
400 2022, 2022.
- Morgenstern, O., Zeng, G., Dean, S. M., Joshi, M., Abraham, N. L., and Osprey, A.: Direct and ozone-mediated forcing of the Southern Annular Mode by greenhouse gases, *Geophysical Research Letters*, 41, 9050–9057, <https://doi.org/10.1002/2014GL062140>, 2014.
- Müller, W., Borchert, L., and Ghosh, R.: Observed Sub-Decadal Variations of European Summer Temperatures, *Geophysical Research Letters*, p. 2019GL086043, <https://doi.org/10.1029/2019GL086043>, 2019.
- 405 Naujokat, B. and Roscoe, H. K.: Evidence against an Antarctic Stratospheric Vortex Split during the Periods of Pre-IGY Temperature Measurements, *Journal of the Atmospheric Sciences*, 62, 885–889, <https://doi.org/10.1175/JAS-3317.1>, 2005.
- Randel, W. J. and Wu, F.: Cooling of the Arctic and Antarctic polar stratospheres due to ozone depletion, *Journal of Climate*, 12, 1467–1479, [https://doi.org/10.1175/1520-0442\(1999\)012<1467:COTAAA>2.0.CO;2](https://doi.org/10.1175/1520-0442(1999)012<1467:COTAAA>2.0.CO;2), 1999.
- Rao, J., Garfinkel, C. I., Wu, T., Lu, Y., and Chu, M.: Mean State of the Northern Hemisphere Stratospheric Polar Vortex in Three Generations
410 of CMIP Models, *Journal of Climate*, 35, 4603–4625, <https://doi.org/10.1175/JCLI-D-21-0694.1>, 2022.
- Reick, C. H., Raddatz, T., Brovkin, V., and Gayler, V.: Representation of natural and anthropogenic land cover change in MPI-ESM, *Journal of Advances in Modeling Earth Systems*, 5, 459–482, <https://doi.org/10.1002/jame.20022>, 2013.
- Rind, D., Suozzo, R., Balachandran, N. K., and Prather, M. J.: Climate Change and the Middle Atmosphere. Part I: The Doubled CO₂ Climate, *Journal of the Atmospheric Sciences*, 47, 475–494, 1990.
- 415 Safieddine, S., Bouillon, M., Paracho, A. C., Jumelet, J., Tencé, F., Pazmino, A., Goutail, F., Wespes, C., Bekki, S., Boynard, A., Hadji-Lazaro, J., Coheur, P. F., Hurtmans, D., and Clerbaux, C.: Antarctic Ozone Enhancement During the 2019 Sudden Stratospheric Warming Event, *Geophysical Research Letters*, 47, 1–10, <https://doi.org/10.1029/2020GL087810>, 2020.
- Shiotani, M. and Hirota, I.: Planetary wave-mean flow interaction in the stratosphere: A comparison between northern and southern hemispheres, *Quarterly Journal of the Royal Meteorological Society*, 111, 309–334, <https://doi.org/10.1002/qj.49711146804>, 1985.
- 420 Solomon, S., Ivy, D. J., Kinnison, D., Mills, M. J., Neely, R. R., and Schmidt, A.: Emergence of healing in the Antarctic ozone layer, *Science*, 353, 269–274, <https://doi.org/10.1126/science.aae0061>, 2016.
- Stolarski, R. S., McPeters, R. D., and Newman, P. A.: The Ozone Hole of 2002 as Measured by TOMS, *Journal of the Atmospheric Sciences*, 62, 716–720, <https://doi.org/10.1175/JAS-3338.1>, 2005.
- Thompson, D. W. J. and Solomon, S.: Interpretation of Recent Southern Hemisphere Climate Change, *Science*, 296, 895–899, <https://doi.org/10.1126/science.1069270>, 2002.
- 425 Thompson, D. W. J. and Solomon, S.: Recent stratospheric climate trends as evidenced in radiosonde data: Global structure and tropospheric linkages, *Journal of Climate*, 18, 4785–4795, 2005.
- Thompson, D. W. J. and Wallace, J. M.: Annular Modes in the Extratropical Circulation. Part I: Month-to-Month Variability*, *Journal of Climate*, 13, 1000–1016, 2000.
- 430 Thompson, D. W. J., Baldwin, M. P., and Solomon, S.: Stratosphere–Troposphere Coupling in the Southern Hemisphere, *Journal of the Atmospheric Sciences*, 62, 708–715, <https://doi.org/10.1175/JAS-3321.1>, 2005.
- Thompson, D. W. J., Solomon, S., Kushner, P. J., England, M. H., Grise, K. M., and Karoly, D. J.: Signatures of the Antarctic ozone hole in Southern Hemisphere surface climate change, *Nature Geoscience*, 4, 741–749, <https://doi.org/10.1038/ngeo1296>, 2011.



435 Wang, L., Hardiman, S. C., Bett, P. E., Comer, R. E., Kent, C., and Scaife, A. A.: What chance of a sudden stratospheric warming in the southern hemisphere?, *Environmental Research Letters*, 15, <https://doi.org/10.1088/1748-9326/aba8c1>, 2020.

World Meteorological Organization (WMO): Scientific assessment of ozone depletion: 2022, WMO, Geneva, *gaw report edn.*, 2022.